A Comparative Molecular Similarity Index Analysis (CoMSIA) study identifies an HLA-A2 binding supermotif

Irini A. Doytchinova & Darren R. Flower
Edward Jenner Institute for Vaccine Research, Compton, Berkshire, RG20 7NN, U.K.

Summary

The 3D-QSAR CoMSIA technique was applied to a set of 458 peptides binding to the five most widespread HLA-A2-like alleles: A*0201, A*0202, A*0203, A*0206 and A*6802. Models comprising the main physicochemical properties (steric bulk, electron density, hydrophobicity and hydrogen-bond formation abilities) were obtained with acceptable predictivity (q^2 ranged from 0.385 to 0.683). The use of coefficient contour maps allowed an A2-supermotif to be identified based on common favoured and disfavoured areas. The CoMSIA definition for the best HLA-A2 binder is as follows: hydrophobic aromatic amino acid at position 1; hydrophobic bulky side chains at positions 2, 6 and 9; non-hydrogen-bond-forming amino acids at position 3; small aliphatic hydrogen-bond donors at position 4; aliphatic amino acids at position 5; small aliphatic side chains at position 7; and small aliphatic hydrophilic and hydrogen-bond forming amino acids at position 8.

Introduction

The T cells are a specialised type of immune cell that mediates cellular immunity [1]. They patrol the body searching for foreign proteins originating from pathogenic organisms. T cells can detect the presence of intracellular pathogens because infected cells display on their surface peptide fragments derived from the pathogens' proteins. These foreign peptides are delivered to the cell surface by specialised host-cell glycoproteins named major histocompatibility complex (MHC) molecules. T cells recognise the peptide–MHC molecule complex and kill the infected cells. The antigen peptides presented to T cells are called epitopes.

There are two classes of MHC molecules. MHC class I molecules deliver peptides originating in the cytosol to the cell surface and are recognised by CD8 T cells. MHC class II molecules deliver peptides originating in the vesicular system to the cell surface, where they are recognised by CD4 T cells. The MHC

class I proteins are encoded by three genetic loci – HLA-A, HLA-B and HLA-C. HLA molecules are extremely polymorphic: the most recent WHO Nomenclature Committee report lists 746 class I alleles [2]. The HLA-A2 family is the largest and most diverse allele family at the HLA-A locus. It consists of 55 alleles and is common in all ethnic groups [3-5]. The most frequent alleles of the HLA-A2 family are A*0201, A*0202, A*0203, A*0206 and A*6802. This set of alleles differ by 1 to 7 amino acids [6], which are centred on the peptide-binding site, and these sequence differences alter the selectivity of peptide binding to the MHC A2 alleles.

X-ray data indicate that the peptide-binding site has a 30Å long surface accessible to a solvent probe [7]. Within this surface, six pockets have been described and denoted A through F. Some of the pockets are non-polar and are expected to form hydrophobic contacts. Others contain polar atoms and could make hydrogen bonds with the side chains of bound peptides. Specific anchor residues that fall into these pockets are thought to mediate peptide binding to MHC molecules. The set of required anchor residues is usually referred to as a motif. Different HLA-A2

*To whom correspondence should be addressed. E-mail: darren.flower@jenner.ac.uk

molecules can recognise very similar peptide binding motifs and this allows the identification of a common motif for the family called a supermotif [3]. Supermotif identification has direct practical implications in the development of epitope-based vaccines for the treatment and prevention of infectious diseases and cancer. Although not all nine amino acids interact strongly with the MHC binding site, all of them contact it [8] and make significant interactions with the MHC molecule. Six of the peptide amino acids fall into the pockets of the binding site; they are defined as primary (positions 2 and 9) and secondary (positions 1, 3, 6 and 7) anchor positions. The remaining three amino acids are accessible to solvent and can also interact with receptors on the T cell. They are able to affect MHC binding affinity in several ways - through direct non-bonded interactions with the MHC, by causing conformational changes in anchor residues, and by altering dynamic properties of the whole peptide.

In the present study we have applied the 3D-QSAR method CoMSIA to peptides which bind the most widespread A2-supertype alleles (A*0201, A*0202, A*0203, A*0206 and A*6802) in order to define a supermotif for the HLA-A2 family. 3D-QSAR methods are attractive for this purpose because of their combination of an understandable molecular description, rigorous statistical analysis, and an unambiguous graphical display of the results [9,10]. They produce quantitatively predictive models, which are far more helpful in the assessment of the binding peptides than use of qualitative descriptors alone. The CoMSIA method uses fields based on similarity indices describing similarities and differences between ligands and correlates them with changes in the binding affinity [11-13]. CoMSIA fields describe steric, electrostatic, hydrophobic and hydrogen-bond donor and acceptor properties. The most important contributions responsible for binding affinity are covered by these properties. Each of them can be visualised in a 3D map denoting the areas, within the binding site, that are 'favoured' or 'disfavoured' by the presence of a group with a particular physicochemical property. Recently, we applied CoMSIA to peptides binding to the HLA-A*0201 allele and obtained a model with good predictivity [14]. Herein, we extend our study to another four A2-supertype alleles. By comparison of the favoured and disfavoured areas, in maps corresponding to the five properties for each allele, we identify a set of common features which allows an extended supermotif to be defined. In contrast to other empirical studies, our

proposed supermotif covers all the 9 positions of the binding nonamer peptides.

Methods

Peptide database

The peptide sequences and their binding affinities were extracted from our recently developed JenPep database [15]. The database is freely accessible from the URL (http://www.jenner.ac.uk/Jenpep). All the peptides included in the study were nonamers. The set of peptides binding to members of the HLA-A2 supertype were: A*0201 (236 peptides), A*0202 (63 peptides), A*0203 (60 peptides), A*0206 (54 peptides), and A*6801 (45 peptides). Some of the peptides bind to more than one allele. The binding affinities (IC_{50}) we used were originally assessed by a quantitative assay based on the inhibition of binding of a radiolabeled standard peptide to detergent-solubilized MHC molecules [16,17] and presented as −log. The magnitude of measured binding affinity ranges over almost 5 orders: from 4.5 to 9.0 in log units.

Molecular modelling

All molecular modelling and QSAR calculations were performed on a Silicon Graphics octane workstation using the SYBYL 6.7 molecular modelling software [18] as previously described [14, 19, 20]. Briefly, the X-ray structure of the nonameric viral peptide TLTSCNTSV [8] bound to HLA-A*0201 molecule was used as a starting conformation for all alleles as there are no X-ray peptide binding data for other A2-supertype alleles. The structures were subjected to fully geometry optimisation using the standard Tripos molecular mechanics force field. The peptide backbone was fixed in the X-ray conformation and kept as an aggregate. The partial atomic charges were computed using the AM1 semiempirical method [21] available in the MOPAC program. MOPAC V6 was used as implemented in SYBYL. Single-point calculations were performed. Molecular alignment was based on the backbone atoms defined as an aggregate in the optimisation process.

CoMSIA Method

CoMSIA was performed using the QSAR option of SYBYL. Five physicochemical properties (steric, electrostatic, hydrophobic, and hydrogen-bond donor

and acceptor) were evaluated, using a common probe atom with 1 Å radius, charge $+1$, hydrophobicity $+1$, hydrogen-bond donor and acceptor properties $+1$. The grid extended beyond the molecular dimensions by 2.0 Å in all directions. Different resolution steps were tested: from 1.0 to 4.0 Å in steps of 0.5 Å. Different column filterings $\sigma_{\min}$ (from 0.0 to 4.0 in steps of 0.5) and attenuation factors α (from 0.1 to 0.8 in steps of 0.1) were analysed as well. The predictive power of the models was assessed by the leave-one-out cross-validated (LOO-CV) coefficient q^2_{LOO}, the standard error of prediction (*SEP*), and the *residuals* between the experimental ($IC_{50\text{exp}}$) and predicted by LOO-CV ($IC_{50\text{pred}}$) binding affinity. According to the *residuals* the peptides were classified into 3 categories: very well predicted peptides with $|residuals| \leq 0.5$ log unit, well predicted peptides with $|residuals|$ between 0.5 and 1.0 and poorly predicted peptides with $|residuals| > 1.0$. A mean $|residual|$ value for the set and its standard deviation were also calculated. More robust cross-validation test was also performed, dividing the sets into 5 groups, developing a number of parallel models from the reduced data with one of the groups omitted, and then predicting the affinities of the excluded peptides. The mean of the q^2 values from 20 runs is given as q^2_{CV5}. As the affinity range for the separate alleles was slightly different, the ratio of the *SEP* to affinity range was used as an additional assessment of the statistical validity of the models. This ratio should be $<10\%$ for good QSAR models [22].

The number of components leading to the highest q^2_{LOO} and the lowest *SEP* defined the optimum number of components (NC) used to derive the non-validated model. The non-cross-validated models were assessed by the explained variance r^2, standard error of estimate (*SEE*), and *F* ratio. This model was used to display the coefficient contour maps. When each field makes a statistical contribution to the predicted binding affinity, the combination of all fields provides the fullest insight into the spatial features of the different fields. In the present study all fields were significant, so only the 'all fields' models for each allele were considered for further analyses.

CoMSIA Maps

The visualisation of the results of the CoMSIA analyses has been performed using the 'StDev*Coeff' mapping option contoured by actual values. The peptide FLLLADARV, which binds to all five HLA-A2 alleles, is shown inside the fields. The contour levels are shown as a colour legend. The contours of the CoMSIA steric map are shown in green (more bulk is favoured) and yellow (less bulk is favoured). The electrostatic map is in red (negative potential is favoured) and blue (negative potential is disfavoured) contours. CoMSIA hydrophobic fields are coloured in yellow (hydrophobic amino acids enhance affinity) and white (hydrophobic groups reduce affinity). Hydrogen bond donor map is in cyan (donors on the ligand are preferred) and purple (donors are disfavoured). In the hydrogen bond acceptor map the favoured areas are shown in magenta, the disfavoured in yellow.

Results

CoMSIA models

In order to generate CoMSIA coefficient contour maps for the A2-supertype alleles considered in the present study, an 'all fields' model was generated for each allele. The results are summarised in Table 1. For the A*0201 allele a recently published model was used (ref. 14, CoMSIA(2)). One hundred and nineteen nonamer peptides binding to 4 other alleles (A*0202, A*0203, A*0306 and A*6802) were built, optimised and AM1 calculations performed within SYBYL. They were placed in a $22 \times 15 \times 15$ grid lattice and aligned based on the backbone atoms. The models were calibrated according to three criteria − grid spacing, attenuation factor α and column filtering. The final settings of the models are shown in Table 1.

The generated models have acceptable predictive ability (q^2_{LOO} ranges from 0.385 to 0.683) and high explained variance (r^2 range is from 0.891 to 0.991). The q^2_{CV5} values are close to the corresponding q^2_{LOO} and this indicates the stability of the models. The ratio *SEP/affinity* range is from 10 to 15%, further substantiating the statistical validity of the models. Peptides with *residuals* below half a log unit constitute between 60 and 73%. The poorly predicted peptides are high for the A*0203 allele (12%) but for the other alleles range from 0 or 4%. Leading contributions made by different fields in the non-cross-validated models are hydrophobic and electrostatic followed by H-bond donor, steric and H-bond acceptor ones.

CoMSIA coefficient contour maps

The non-cross-validated models were used to generate the coefficient contour maps. Peptide FLLLADARV is
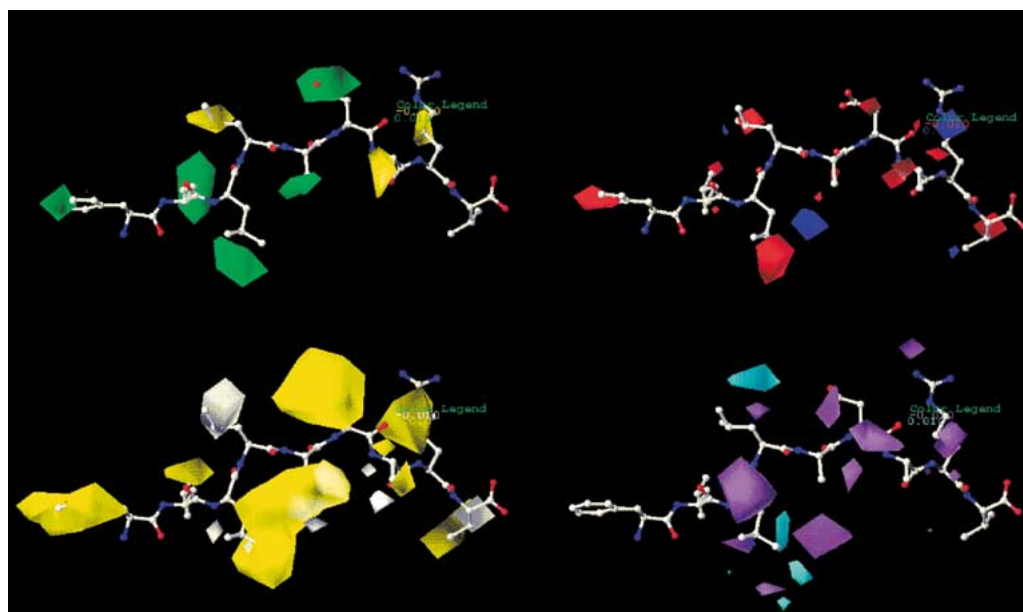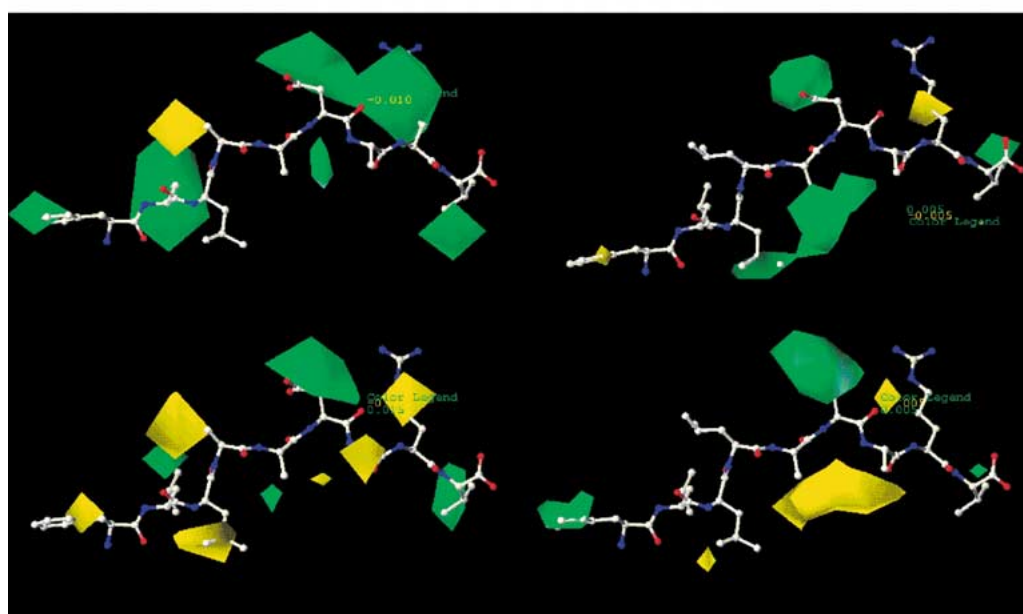
Figure 1. (a) CoMSIA stdev*coeff contour plots for A*0201. Peptide FLLLADARV is shown inside the fields, N terminal is positioned on the left side. Upper left: steric map. Green and yellow polyhedra indicate regions where steric bulk will enhance or decrease the affinity, respectively. Upper right: electrostatic map. Red and blue polyhedra indicate regions where electron density will enhance or decrease the affinity, respectively. Lower left: hydrophobic map. Yellow and white polyhedra indicate regions where hydrophobicity will enhance or decrease the affinity, respectively. Lower right: H-bond donor ability. Cyan and purple polyhedra indicate regions where H-bond donors on the ligand will enhance or decrease the affinity, respectively. The map of H-bond acceptor ability is not shown. Favoured H-bond acceptor areas exist at P4 and P8, disfavoured – at P2, P3, P5, P6 and P7. (b) Steric CoMSIA stdev*coeff contour plots. Peptide FLLLADARV is shown inside the fields, N terminal is positioned on the left side. Upper left: A*0202. Upper right: A*0206. Lower left: A*0203. Lower right: A*6802. Green and yellow polyhedra indicate regions where steric bulk will enhance or decrease the affinity, respectively.
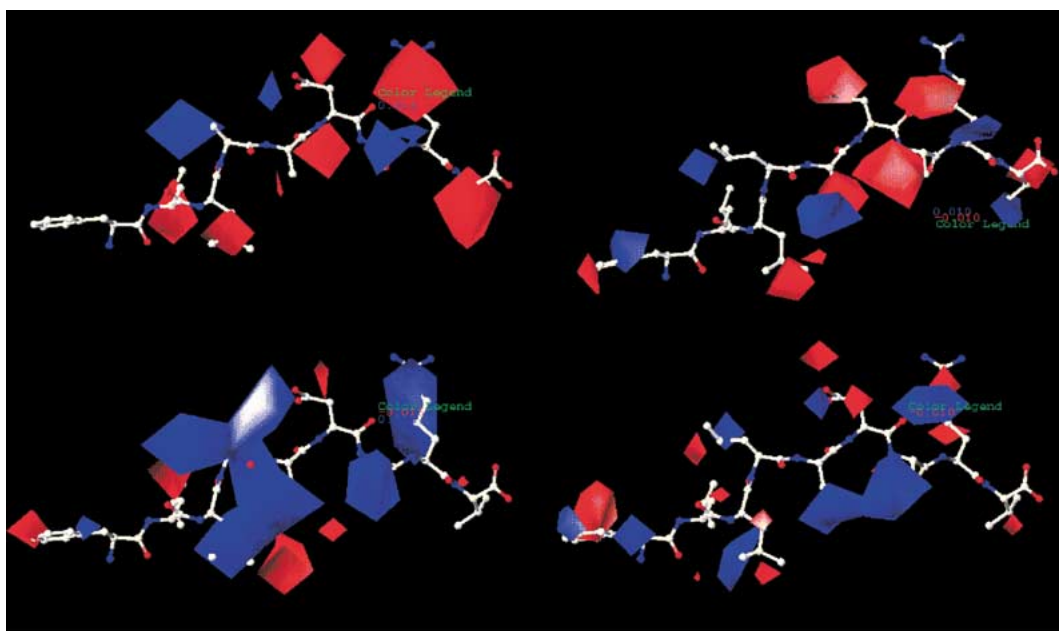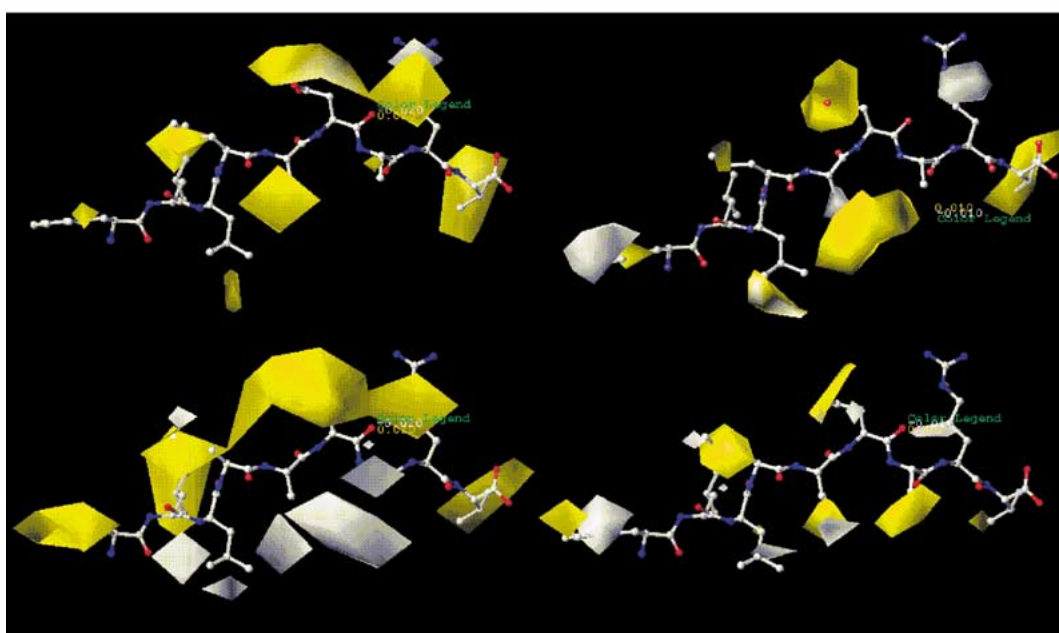
Figure 2. (a) Electrostatic CoMSIA stdev*coeff contour plots. Peptide FLLLADARV is shown inside the fields, N terminal is positioned on the left side. Upper left: A*0202. Upper right: A*0206. Lower left: A*0203. Lower right: A*6802. Red and blue polyhedra indicate regions where electron density will enhance or decrease the affinity, respectively. (b) Hydrophobic CoMSIA stdev*coeff contour plots. Peptide FLLLADARV is shown inside the fields, N terminal is positioned on the left side. Upper left: A*0202. Upper right: A*0206. Lower left: A*0203. Lower right: A*6802. Yellow and white polyhedra indicate regions where hydrophobicity will enhance or decrease the affinity, respectively.

Table 1. CoMSIA models.

Parameter	A*0201		A*0202		A*0203		A*0206		A*6802	
n	236		63		60		54		45	
q^2_{LOO}	0.683		0.534		0.621		0.523		0.385	
q^2_{CV5}	0.656		0.467		0.572		0.466		0.366	
NC	7		8		6		12		4	
SEP	0.443		0.509		0.595		0.505		0.652	
SEP/affinity range (%)	10		14		13		13		15	
r^2	0.891		0.935		0.966		0.991		0.944	
SEE	0.260		0.190		0.179		0.071		0.197	
F ratio	265.082		97.199		247.303		363.764		168.149	
Settings:										
Grid spacing (Å)	2.0		3.0		3.0		2.0		2.0	
Attenuation factor	0.5		0.4		0.4		0.3		0.5	
Column filtering	2.0		0.5		0.5		0.5		3.0	
Fractions:										
Steric	0.145		0.144		0.162		0.110		0.114	
Electrostatic	0.320		0.228		0.177		0.282		0.265	
Hydrophobic	0.210		0.291		0.270		0.304		0.260	
H-bond donor	0.161		0.210		0.235		0.210		0.214	
H-bond acceptor	0.164		0.127		0.157		0.094		0.148	
Residuals:										
res. ≤ |0.5|	166	70%	42	67%	44	73%	36	63%	27	60%
|0.5| < *res.* ≤ |1.0|	70	30%	21	33%	9	15%	19	33%	16	36%
res. > |1.0|	0	0%	0	0%	7	12%	2	4%	2	4%
mean |residual|	0.340		0.393		0.434		0.443		0.519	
st dev	0.246		0.281		0.356		0.310		0.332	

shown inside the fields. Maps corresponding to the five different field types were created to describe the relationships between the binding affinity and the steric bulk, the electron density, the local hydrophobicity, the hydrogen-bond donor and acceptor abilities. Four of the five physicochemical properties for A*0201 allele are shown in Figure 1a. The maps for the other A2-supertype alleles are shown in Figures 1b-3.

Steric bulk. The steric map for the A*0201 allele is shown in Figure 1a (upper left) and for the A*0202, A*0203, A*0206 and A*6802 alleles in Figure 1b. Steric bulk at position 6 (P6) is favoured for all of the alleles. At position 9 (P9) it is favoured for 4 alleles (A*0202, A*0203, A*0206 and A*6802) and at position 2 (P2) for 3 alleles (A*0201, A*0202 and A*0203). At position 1 (P1) steric bulk is favoured for A*0201, A*0202 and A*6802 but it is disfavoured for A*0203. At position 5 (P5) steric bulk is favoured for A*0201, A*0202 and A*0206 but it is disfavoured for A*6802. At position 3 (P3) the ratio of favoured to

disfavoured is 2:1 (favoured for A*0201 and A*0206 and disfavoured for A*0203). Disfavoured steric bulk exists at positions 4 (P4) for A*0201, A*0202 and A*0203 and at position 7 (P7) for A*0201, A*0203 and A*6802. At position 8 (P8) steric bulk is disfavoured for all alleles except of A*0202.

Electron density. Great diversity exists in the electrostatic maps of A2-supertype alleles (Figures 1a, upper right, and 2a). Areas where electron density is favoured could be associated with aromatic or heteroatom-bearing side chains. Contrariwise, the disfavoured electron density suggests a preference for aliphatic groups. Many of the side chains bear favoured negative potential areas as well as disfavoured ones. Increased electron density is well accepted at P3 and P6, but not at P4.

Hydrophobicity. For most of the A2-supertype alleles hydrophobic side chains are well accepted at P2, P6 and P9 (Figures 1a, lower left, and 2b). For three of the

five alleles (A*0202, A*0206 and A*6802) hydrophobic side chains at P8 are not favoured. Hydrophobicity at P1 is preferred for A*0201, A*0202 and A*0203 alleles but not for A*0206 and A*6802. There is not a well-defined hydrophobic preference at the other positions.

Hydrogen-bond donor and acceptor abilities. There are many favoured areas for H-bond donor groups but only two are common for three or more alleles: those at P4 and P8 (Figures 1a, lower right, and 3a). There is only one favoured area common to all five alleles in the H-bond acceptor maps: at P8 (Figure 3b).

Discussion

A great advantage of 3D-QSAR methods is their ability to generate contour maps that display areas that are favourable or disfavourable for activity. This display is easily interpreted by non-computational scientists and is well suited to design purposes [9, 10]. But the power of these maps should not be magnified unduly – they do not pin point the pharmacophore, rather they show only where changes in the structure produce changes in biological potency.

In the present study CoMSIA models were generated to reveal the importance of five physicochemical properties for the binding affinity to five A2-like alleles in order to define a supermotif. For a better interpretation of the results, coefficient contour maps were generated for each property and for each allele and common requirements were defined for each position in the binding nonamer peptide. In accordance with accepted terminology the areas were identified as preferred (favoured) and deleterious (disfavoured) [23]. Areas identified as favoured for three or more A2-supertype molecules, without being disfavoured for any molecule, may be considered as preferred for the supermotif. Areas identified as disfavoured for three or more molecules can be considered as deleterious in the common motif. Position specificities are presented in Table 2.

Hydrophobic aromatic amino acids at P1 and hydrophobic bulky side chains at P2 are preferred for the A2-supermotif. This is in a good agreement with many experimental data [24–29] and with Sette's consensus A2-supermotif [23]. The side chains of P1 and P2 fall into pockets A and B, respectively [30]. At P3 non-hydrogen-bond forming amino acids are preferred. The side chain of P3 falls into pocket D [30].

Small aliphatic H-bond donors are well accepted at P4. The only requirement for the residue at P5 is to be aliphatic. For the remaining four positions the preferences are as follows: hydrophobic and bulky at P6 and P9, small and aliphatic at P7, and small, aliphatic, hydrophilic, and hydrogen-bond forming amino acids at P8. Side chains of P6, P7 and P9 fall into pockets C, E and F, respectively [30]. P4 and P8 are called 'flag' residue [7] because they are solvent-exposed in the complex with MHC molecule and can therefore contact T cell receptors.

There are two A2-supermotifs already defined in the literature. The oldest is Sette's 'L_2V_9' [31] based on preferred aliphatic residues at P2 and P9. Recently, this motif was extended to cover some of the secondary anchor positions: P1 and P3 [23]. It was found that aromatic residues were commonly preferred at P1 and an aversion to charged residues (Arg, Lys, Asp and Glu) at P3 was also noted. It was also noted that preferences at P2 for the A*6802 allele and the set of A*02 alleles were different: Val and Thr are preferred for A*6802, Leu and Met for A*0201 and A*0203, and Gln for A*0202 and A*0206 [20]. Applying a Free-Wilson additive method [32] to peptides binding to HLA-A2-like alleles confirmed this difference.

In CoMSIA, steric and hydrophobic maps at P2 for A*0206 and A*6802 alleles remain silent – neither favoured nor disfavoured areas exist here. The preferred hydrophobic bulky substituent in the A2-supermotif is defined on the basis of the other three alleles – A*0201, A*0202 and A*0203. It is well known that the side chain of P2 falls into pocket B of the binding cleft [30]. The comparison of residues forming the B pocket in the different alleles showed that Phe is available at position 9 in A*0201, A*0202 and A*0203 but Tyr in A*0206 and A*6802 [33]. The Phe9 $\rightarrow$ Tyr9 substitution makes the pocket shallow and long side chains, such as Leu and Met, can no longer be accommodated here. Molecular modelling studies hypothesise a possible conformational shift of the aromatic ring of Tyr9 into the cavity [34]. This conformational change would narrow the size of the B pocket and weaken the entirely hydrophobic nature of this pocket.

Motif definition is a requirement for the initial *in silico* step of epitope identification [5]. The more precisely a motif is defined the greater the accuracy of epitope prediction. In this sense, a quantitative prediction is more helpful than a qualitative description. As a quantitative method CoMSIA allows quantitative predictions and assessment of potential good binders.
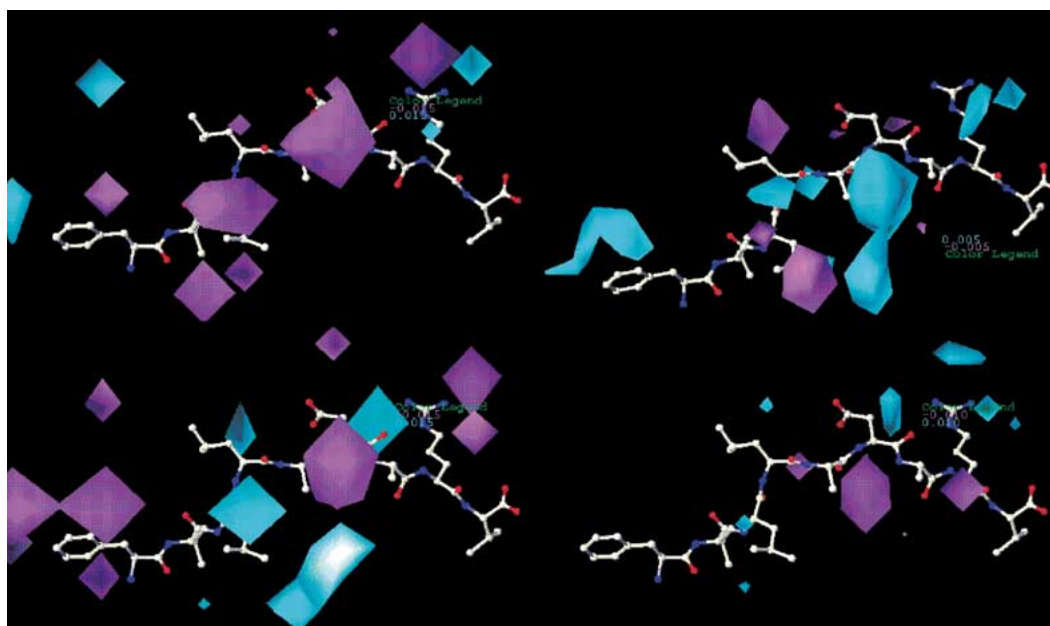
a
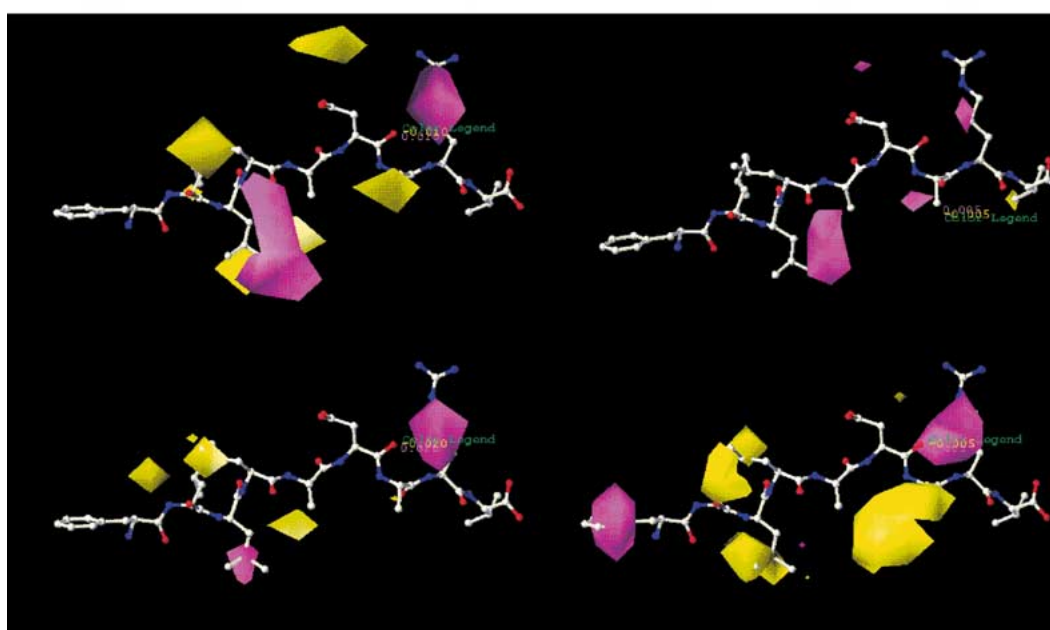
b

Figure 3. (a) Hydrogen-bond donor CoMSIA stdev*coeff contour plots. Peptide FLLLADARV is shown inside the fields, N terminal is positioned on the left side. Upper left: A*0202. Upper right: A*0206. Lower left: A*0203. Lower right: A*6802. Cyan and purple polyhedra indicate regions where H-bond donors will enhance or decrease the affinity, respectively. (b) Hydrogen-bond acceptor CoMSIA stdev*coeff contour plots. Peptide FLLLADARV is shown inside the fields. Upper left: A*0202. Upper right: A*0206. Lower left: A*0203. Lower right: A*6802. Magenta and yellow polyhedra indicate regions where H-bond acceptors will enhance or decrease the affinity, respectively.

Table 2. A2 supermotif.

Position	Steric bulk	Electron density	Hydrophobicity	H-bond donor	H-bond acceptor
Position 1 (P1) Side chain falls into pocket A.		Favoured. Aromatic amino acids are preferred.	Favoured.		
Position 2 (P2) Side chain falls into pocket B.	Favoured.		Favoured.		Disfavoured.
Position 3 (P3) Side chain falls into pocket D.				Disfavoured	Disfavoured
Position 4 (P4) Side chain is solvent-exposed and can contact T cell.	Disfavoured	Disfavoured Aliphatic amino acids are preferred.		Favoured.	Disfavoured
Position 5 (P5)		Disfavoured Aliphatic amino acids are preferred.			
Position 6 (P6) Side chain falls into pocket C.	Favoured.		Favoured.		Disfavoured.
Position 7 (P7) Side chain falls into pocket E.	Disfavoured.	Disfavoured Aliphatic amino acids are preferred.			Disfavoured
Position 8 (P8) Side chain is solvent-exposed and can contact T cell.	Disfavoured.	Disfavoured. Aliphatic amino acids are preferred.	Disfavoured.	Favoured.	Favoured.
Position 9 (P9) Side chain falls into pocket F.	Favoured.		Favoured.		

This affects the amount of subsequent experimental work as well as the risk of false negative predictions. Defining a supermotif also allows identification of epitopes that can simultaneously, or promiscuously, bind a number of alleles. Identification of such promiscuous binders is a powerful extension to established epitope-based vaccine design. The development of such vaccines is likely to prove of great utilitarian value in the treatment and prevention of allergy, cancer, autoimmune and infectious diseases.

Conclusions

CoMSIA has been successfully applied to the identification of a supermotif for five HLA-A2-like alleles: A*0201, A*0202, A*0203, A*0206 and A*6802. Preferred and deleterious areas of steric bulk, electron density, local hydrophobicity and hydrogen-bond forming properties for each position of the binding nonamer peptides were defined. We anticipate that this expanded definition of the HLA-A2 supermotif will demonstrate significant utility in the on going search for new epitope-based vaccines.

544

References

1. Janeway, C. A. Jr., Travers, P., Walport, M. and Capra, J. D. (Eds.), Immunobiology, Elsevier Science Ltd., London, 1999, pp. 115–162.
2. Marsh, S. G. E., Bodmer, J. G., Albert, E. D., Bodmer, W. F., Bontrop, R. E., Dupont, B., Erlich H. A., Hansen, J. A., Mach, B., Mayr, W. R., Parham, P., Petersdorf, E. W., Sasazuki, T., Schreuder G. M. Th., Strominger, J. L., Svejgaard, A. and Terasaki, P. I., Eur. J. Immunogenet., 28 (2001) 377.
3. Sidney, J., Grey, H. M., Kubo, R. T. and Sette, A., Immunol. Today, 17 (1996) 261.
4. Ellis, J. M., Henson, V., Slack, R., Ng, J., Hartzman, R. J. and Hurley, C. K., Hum. Immunol., 61 (2000) 334.
5. Sette, A., Livingston, B., McKinney, D., Appella, E., Fikes, J., Sidney, J., Newman, M. and Chesnut, R., Biologicals 29 (2001) 271.
6. Schönbach, C., Koh, J. L. Y., Sheng, X., Wong, L. and Brusic, V., Nucleic Acids Res. 28 (2000) 222.
7. Madden, D. R., Annu. Rev. Immunol. 13 (1995) 587.
8. Madden, D. R., Garboczi, D. N. and Willey, D. C., Cell 75 (1993) 693.
9. Oprea, T. I. and Waller, C. L., In Lipkowitz, K. B. and Boyd, D. B. (Eds.), Reviews in Computational Chemistry, Volume 11, Wiley-VCH, New York, 1997, pp. 127–182.
10. Greco, G., Novellino, E. and Martin, Y. C, In Lipkowitz, K. B. and Boyd, D. B. (Eds.), Reviews in Computational Chemistry, Volume 11, Wiley-VCH, New York, 1997, pp. 183–240.
11. Klebe, G., Abraham, U. and Mietzner, T., J. Med. Chem. 37 (1994) 4130.
12. Klebe, G. and Abraham, U., J. Comput.-Aid. Mol. Des. 13 (1999) 1.
13. Böhm, M., Stürzebecher, J. and Klebe, G., J. Med. Chem. 42 (1999) 458.
14. Doytchinova, I. A. and Flower, D. R., PROTEINS 48 (2002) 505.
15. Blythe, M. J., Doytchinova, I. A. and Flower, D. R., Bioinformatics 18 (2002) 434.
16. Ruppert, J., Sidney, J., Celis, E., Kubo, R. T., Grey, H.M. and Sette, A., Cell 74 (1993) 929.
17. Sette, A., Sidney, J., del Guercio, M.-F., Southwood, S., Ruppert, J., Dalberg, C., Grey, H. M. and Kubo, R. T., Mol. Immunol. 31 (1994) 813.
18. SYBYL 6.7. Tripos Inc., 1699 Hanley Road, St. Louis, MO 63144.
19. Doytchinova, I. A. and Flower D. R., J. Med. Chem. 44 (2001) 3572.
20. Doytchinova, I. A. and Flower D. R., Immunol. Cell Biol. 80 (2002) 270.
21. Dewar, M. J. S., Zoebisch, E. G., Healy, E.F. and Stewart, J. J. P., J. Am. Chem. Soc. 107 (1985) 3902.
22. Apex-3D 95.0. User Guide, Biosym/MSI, 9685 Scranton Road, San Diego, CA 92121.
23. Sidney, J., Southwood, S., Mann, D. L., Fernandez-Vina, M. A., Newman, M. J. and Sette A., Hum. Immunol. 62 (2001) 1200.
24. Kirksey, T. J., Pogue-Caley, R. R., Frelinger, J. A. and Collins, E. J., J. Biol. Chem. 274 (1999) 37259.
25. Tourdot, S., Scardino, A., Saloustrou, E., Gross, D. A., Pascolo, S., Cordopatis, P., Lemonnier, F. A. and Kosmatopoulos, K. A., Eur. J. Immunol. 30 (2000) 3411.
26. Ruppert, J., Sidney, J., Celis, E., Kubo, R. T., Grey, H. M. and Sette, A., Cell 74 (1993) 929.
27. Parker, K. C., Bednarek, M. A. and Coligan, J.E., J. Immunol. 152 (1994) 163.
28. Kubo, R. T., Sette, A., Grey, H. M., Appella, E., Sakaguchi, K., Zhu, N.-Z., Arnott, D., Sherman, N., Shabanowitz, J., Michel, H., Bodnar, W. M., Davis, T. A. and Hunt, D. F., J. Immunol. 152 (1994) 3913.
29. Parker, K. C., Bednarek, M. A., Hull, L. K., Utz, U., Cunningham, B., Zweerink, H. J., Biddison, W. E., Coligan, J. E., J. Immunol. 149 (1992) 3580.
30. Saper, M. A., Bjorkman, P. J. and Wiley, D. C. J. Mol. Biol. 219 (1991) 277.
31. Del Guercio, M.-F., Sidney, J., Hermanson, G., Perez, C., Grey, H. M., Kubo, R. T. and Sette, A., J. Immunol. 154 (1995) 685.
32. Doytchinova, I. A., Blythe, M. J. and Flower, D. R., J Proteome Res. 1 (2002) 263.
33. Schönbach, C., Koh, J. L. Y., Sheng, X., Wong, L. and Brusic, V., Nucleic Acids Res. 28 (2000) 222.
34. Sudo, T., Kamikawaji, N., Kimura, A., Date, Y., Savoie, C. J., Nakashima, H., Furuichi, E., Kuhara, S. and Sasazuki, T., J. Immunol. 155 (1995) 4749.